



# Photoinduced control of ferroelectricity in hybrid-improper ferroelectric superlattices

Lingyuan Gao, Laurent Bellaiche, Charles Paillard

## ► To cite this version:

Lingyuan Gao, Laurent Bellaiche, Charles Paillard. Photoinduced control of ferroelectricity in hybrid-improper ferroelectric superlattices. *Physical Review B*, 2023, 107 (10), pp.104109. 10.1103/PhysRevB.107.104109 . hal-04057967

**HAL Id: hal-04057967**

**<https://centralesupelec.hal.science/hal-04057967>**

Submitted on 4 Apr 2023

**HAL** is a multi-disciplinary open access archive for the deposit and dissemination of scientific research documents, whether they are published or not. The documents may come from teaching and research institutions in France or abroad, or from public or private research centers.

L'archive ouverte pluridisciplinaire **HAL**, est destinée au dépôt et à la diffusion de documents scientifiques de niveau recherche, publiés ou non, émanant des établissements d'enseignement et de recherche français ou étrangers, des laboratoires publics ou privés.

# Photo-induced control of ferroelectricity in hybrid-improper ferroelectric superlattices

Lingyuan Gao,<sup>1</sup> Charles Paillard,<sup>2</sup> and Laurent Bellaïche<sup>1</sup>

<sup>1</sup>*Physics Department and Institute for Nanoscience and Engineering,  
University of Arkansas, Fayetteville, Arkansas, 72701, USA*

<sup>2</sup>*Université Paris-Saclay, CentraleSupélec, CNRS,  
Laboratoire SPMS, 91190, Gif-sur-Yvette, France.*

(Dated: January 16, 2023)

We reveal a photo-induced control of ferroelectricity in hybrid-improper ferroelectric superlattices, using *ab-initio* theory. Along with a notable photostriction effect, thermalized carriers from photo-excitation affect octahedral tiltings along different directions. A trilinear coupling between antipolar and tilting modes drives corresponding cationic displacements, and this results in a **decrease** in polarization under light. Together with recent experimental evidences, our study therefore demonstrates that light is a viable route to engineer functionalities in materials.

With spontaneous and switchable electric polarizations, ferroelectrics (FEs) have important implications not only in fundamental science but also in device applications. Conventional ferroelectricity, such as in perovskite oxides  $\text{BaTiO}_3$ , is attributed to a  $p$ - $d$  hybridization between Ti  $d^0$  and oxygen  $p$  states, where the long-range Coulomb forces are favored against the short-range repulsion [1]. As a result, Ti off-centering displacement in  $\text{BaTiO}_3$  is induced, which breaks the centrosymmetry. With a different origin, the “hybrid improper” ferroelectricity, identified in perovskite superlattices such as  $\text{ABO}_3/\text{A}'\text{BO}_3$  and layered perovskites  $(\text{ABO}_3)_2(\text{AO})$  [2–4], arises from a trilinear coupling between a polar mode on A sites and two non-polar tilting modes of  $\text{BO}_6$  octahedra. The mechanism relies more on the geometry of the lattice (namely, the non-full compensation between antipolar displacements of A cations on different layers) rather than on the electrostatic forces as in conventional FE [5, 6].

Different approaches have been proposed to manipulate ferroelectricity. Strains applied on thin films can affect the electric polarization of  $\text{BaTiO}_3$ , and can also render the quantum paraelectric  $\text{SrTiO}_3$  ferroelectric and even increase its transition temperature [7, 8]. Charge doping has been demonstrated to be another effective manner to tune ferroelectricity and create novel phases. In conventional FE such as  $\text{LiNbO}_3$  and  $\text{BaTiO}_3$ , the ferroelectric displacement can be suppressed by increasing the number of doped carriers [9–12]. While in the **trilinear** Ruddlesden-Popper phase of layered perovskites, a very recent study shows that in  $\text{A}_3\text{Sn}_2\text{O}_7$  electrostatic doping leads to an increase of octahedral rotation [13], which then enhances the polarization. Since carriers can screen the long-range interaction and have a tendency to preserve the centrosymmetry, it is counterintuitive that ferroelectricity coexists with metallicity. Such unusual coexistence had not been discovered until 2013, when  $\text{LiOsO}_3$  was identified as the first “polar metal” [14]—six decades after its theoretical prediction [15]. More recent works show that the 2D topological semimetal  $\text{WTe}_2$  also displays a switchable polarization [16].

Alternatively, with the advancement of optical pumping, intense irradiation by ultrafast laser pulses has become another method to trigger novel phase transitions. It is not only limited to the low-frequency or THz dynamical process where phonons are resonantly excited to drive the system [17–20]. By absorbing photons, photo-excited electrons at quasi-equilibrium condition can reshape the potential energy landscape and induce structural distortions, which are rarely visited otherwise. Photo-induced phase transitions have been predicted [21] and realized in FEs [22]; recently, it has been revealed that optical excitation can induce an increasing octahedral tilting in Ca-doped  $\text{SrTiO}_3$  and  $\text{EuTiO}_3$  [23, 24]. Charge ordered phases can also form after the illumination of light in  **$\text{LaTe}_3$ ,  $\text{MoTe}_2$  and  $\text{WTe}_2$**  [25, 26].

In this work, using first-principle calculations **to simulate the effect of photo-excited carriers**, we show the pivotal role of light illumination in controlling the electric polarization of hybrid improper ferroelectrics (HIFs). Intuitively, photo-excited carriers should screen the electric polarization as a response to the intrinsic electric field. Instead in HIFs, at quasi-equilibrium state, photo-excited carriers tailor the polarization by governing tilting modes of octahedra via trilinear coupling [2–4]. This is in contrast to electrostatical doping in conventional FEs, where carriers screen the long-range Coulomb force and reduce the ferroelectric off-centering displacement [10, 11]. As an example, by choosing the prototypical HIF superlattice  $\text{LaGaO}_3/\text{YGaO}_3$ , we show how tiltings increase and antipolar displacements concomitantly get enhanced, but polarization decreases with the intensity of illumination. **This is because though light renders larger displacements of La and Y as a result of the enhancement of tiltings, two cations move antiparallel to each other; with their magnitudes becoming closer under illumination of higher intensity, the net polarization decreases as a result. This is different from  $\text{PbTiO}_3$ , where the polar instability is directly suppressed by enhanced tilting instabilities under photo-illumination [21].** The polarization change occurs concurrently with a photo-induced volume expansion, known as photostriction effect [27–29].

**Methodology** When an insulator is irradiated by above-bandgap photons, dynamics of excited carriers can be divided into three stages: photoexcitation, thermalization, and recombination [30, 31]. By absorbing photon energy, electrons are pumped to occupy conduction bands and leave holes in valence bands. With electron-electron/hole-hole interaction, two types of carriers will reach quasi-equilibrium where the population follows a Fermi-Dirac distribution with well-defined carrier temperatures. The excitation and carrier-carrier interaction happen at a femtosecond-time-scale [32–34]. Redistributed electrons and holes on conduction bands and valence bands will reshape the potential energy surface, and the restoring forces will drive fast atomic motions [35, 36]. It can not only be resolved in experiments but also can be distinguished from subsequent events such as heat transfer from electrons to lattice due to electron-phonon interaction and phonon decay at a longer timescale [23, 36]. The above mentioned processes still have shorter timescales compared to the recombination process at the nanosecond level [32, 37]. All dynamical processes are illustrated in Fig. 1(a). Here we focus on the transient state after photo-excitation and before heat transfer, where carriers have reached quasi-equilibrium, and atoms are well relaxed by interatomic forces. This state can be created by a pulsed laser.

This transient state can be described using constrained density functional theory (DFT) calculations [38, 39], where the intensity of illumination can be converted to the number of photo-excited electron-hole pairs,  $n_{ph}$ , via:

$$\eta JS_0 = \frac{d}{a_0} \Delta_{gap} n_{ph}. \quad (1)$$

$\eta$  denotes the conversion efficiency while  $J$  denotes the energy fluence of one laser pulse.  $a_0$ ,  $S_0$  denote the out-of-plane lattice constant and area of one formula unit (f.u.) of the cell, respectively. With  $\Delta_{gap} = 4$  eV as the indirect bandgap predicted by DFT for  $\text{LaGaO}_3/\text{YGaO}_3$  (see Fig. S2 in Supplementary Materials (SM)), if we take  $\eta = 25\%$  (which is close to photo-conversion efficiency of a solar cell), for a thin film with thickness  $d = 10$  nm, the number of photo-excited carriers  $n_{ph}$  is 0.44 e/f.u. for a homogeneous illumination of  $J = 10$  mJ/cm<sup>2</sup> – which is accessible for contemporary pulsed lasers. As a sound estimate, we thus vary  $n_{ph}$  in the range of 0–1 e/f.u.. Since we are not focusing on carrier dynamics, methods such as time-dependent density functional theory (TDDFT) used elsewhere are not considered [23, 24].

We adopt the conventional cell containing four superlattice formula units so that octahedral tilting pattern can be fully displayed (shown in Fig. 1(b)). With  $a^-a^-c^+$  in Glazer notation [40], the tiltings are out-of-phase along in-plane axes but in phase along the out-of-plane axis. In the presence of photo-excited carriers, we perform structural relaxation including both atomic

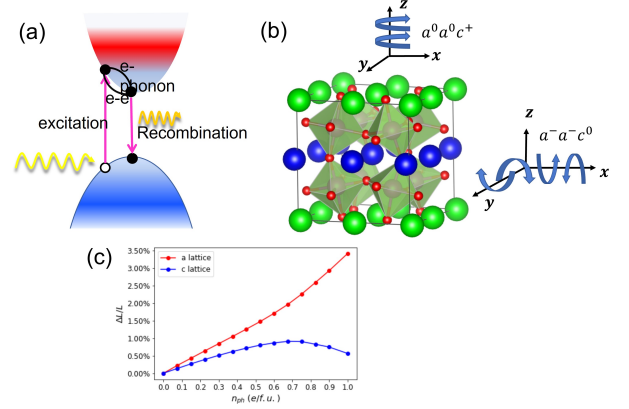


FIG. 1. (a) Three dynamic events electrons experience after illumination, including photo-excitation, electron-electron/electron-phonon interaction, and electron-hole recombination. (b) Illustration about out-of-plane, in-phase tilting  $c^+$  and in-plane, out-of-phase tilting  $a^-$  in  $\text{LaGaO}_3/\text{YGaO}_3$ . Two arrows indicate tilting directions of octahedra in front and rear layers around respective axis, respectively. (c) Photo-induced strain for in-plane  $a$  and out-of-plane  $c$  lattice constants as a function of photo-excited carriers  $n_{ph}$ .

coordinates and lattice using the plane-wave DFT code Abinit [41]. Other details of calculations can be found in SM.

**Photostriction and photo-induced polarization** We first look at the photostriction effect, namely, photo-induced lattice change in  $\text{LaGaO}_3/\text{YGaO}_3$ . Figure 1(c) shows that the in-plane lattice constant expands with the injection of photo-excited carriers, and the increase is up to 3.5% when  $n_{ph} = 1$  e/f.u.. The out-of-plane lattice constant first increases by 0.9% when  $n_{ph} = 0.7$  e/f.u. and then gradually decreases. Similar effect has been observed in halide perovskites, which has been attributed to the character of electrons excited by photons with different energies [42]. Photostriction in the HIF superlattice is much more pronounced than the one predicted by the  $\Delta\text{SCF}$  method in  $\text{BaTiO}_3$  [28], and with the same order of magnitude as in  $\text{PbTiO}_3$  and  $\text{BiFeO}_3$  [27, 28]. The compressive photo-induced strain in conventional FEs and multiferroics are explained by a converse piezoelectric effect, where screening and resulting reduction of polarization from illumination lead to a shrinking of lattice constant [27, 28]. With a different origin, here we associate the tensile, photo-induced strain in HIF with a weaker Ga-O bonding and an elongated Ga-O bond length, so as to lower the energy of the bonding and anti-bonding states occupied by thermalized holes and electrons, respectively (details are provided in the SM).

Polar displacements have been widely used to characterize the ferroelectricity in polar metals and doped systems [10, 11, 13, 43]. As in Refs. [13], the effective po-

larization  $\vec{P}$  is computed as the sum of atomic displacements from high symmetry positions times the respective Born effective charges (see SM for more details). Since we consider a small number of photo-excited carriers, we take the Born effective charges to be the same before and after illumination. Figure 2(a) shows the variation of the total polarization,  $P$ , with  $n_{ph}$ .  $P$  decreases linearly before the turning point  $n_{ph} = 0.6$  e/f.u., at which the out-of-plane lattice constant also changes its behavior as shown in Fig. 1(c). After that,  $P$  decreases at a more rapid rate. At  $n_{ph} = 1$  e/f.u., it arrives at  $10.9 \mu\text{C}/\text{cm}^2$ , reducing by 12% from its original value. To determine the contribution from each atomic species, we decompose the  $x$ -component of the polarization  $P_x$  into  $P_x^{\text{LaY}}$ ,  $P_x^{\text{Ga}}$  and  $P_x^{\text{O}}$ , which originate from displacements of cations on A-site, Ga and of oxygens, respectively. We note that the components of the polarization along  $x$  and  $y$  directions are almost identical (see Fig. S3 in SM) and the component along  $z$  direction  $P_z$  is almost 0, indicating that the total polarization is along the  $[-1-10]$  direction, typical of HIF systems [44, 45]. As shown in Fig. 2(b), the polarization in  $\text{LaGaO}_3/\text{YGaO}_3$  superlattice is largely contributed by cations on A-sites for the dark condition  $n_{ph} = 0$ . This results from the anti-polar displacements between  $\vec{D}_{\text{La}}$  and  $\vec{D}_{\text{Y}}$  driven by two unstable non-polar octahedral tiltings  $a^0a^0c^+$  and  $a^-a^-c^0$  [4], and it constitutes over 50% of the total polarization. With  $\vec{D}_{\text{La}} \neq -\vec{D}_{\text{Y}}$ , oxygen displacements at LaO and YO layers related with  $a^-a^-c^0$  tilting are also asymmetric, and that contributes partially to  $P_x$  and  $P_y$  too. By turning on the light,  $P_x^{\text{LaY}}$  from A-site anti-polar mode increases significantly, while  $P_x^{\text{Ga}}$  becomes more negative. Overall three contributions therefore give rise to a less negative  $P_x$  and a smaller  $P$  with an increasing  $n_{ph}$ .

To elucidate the origin of the polarization change under illumination, we plot the  $\phi_{a^-}$  antiphase tilting angle and the  $\phi_{c^+}$  inphase tilting angle as a function of  $n_{ph}$  in Fig. 2(c). We find increase on both  $\phi_{a^-}$  and  $\phi_{c^+}$ , but the increase of  $\phi_{c^+}$  is more remarkable. The tiltings are enhanced by the photo-excited carriers. Nevertheless, in stark contrast to the previously studied layered perovskite  $\text{A}_3\text{Sn}_2\text{O}_7$  with electrostatic doping [13], a large amplitude of tilting does not imply of a larger polarization. This is because previous atomistic theories reveal that the antipolar displacement  $\vec{D}_{\text{Y}} - \vec{D}_{\text{La}}$ , rather than the polar displacement  $\vec{D}_{\text{Y}} + \vec{D}_{\text{La}}$  (which is directly linked to polarization), is proportional to the product of the two tilting angles [45, 46]:

$$D_x^{\text{Y}} - D_x^{\text{La}} \propto \phi_{a^-} \phi_{c^+} (K^{\text{Y}} + K^{\text{La}}). \quad (2)$$

Here,  $K$  denotes the coupling coefficient between in-plane atomic displacements and tilting modes, and  $K^{\text{Y}}$  and  $K^{\text{La}}$  have the same sign. To show this correlation, we plot  $D_x^{\text{Y}}$ ,  $D_x^{\text{La}}$  and  $D_x^{\text{Y}} - D_x^{\text{La}}$  vs  $n_{ph}$  in Fig. 2(d). Indeed, following enhanced tiltings,  $D_x^{\text{Y}}$  and  $D_x^{\text{La}}$  (that are

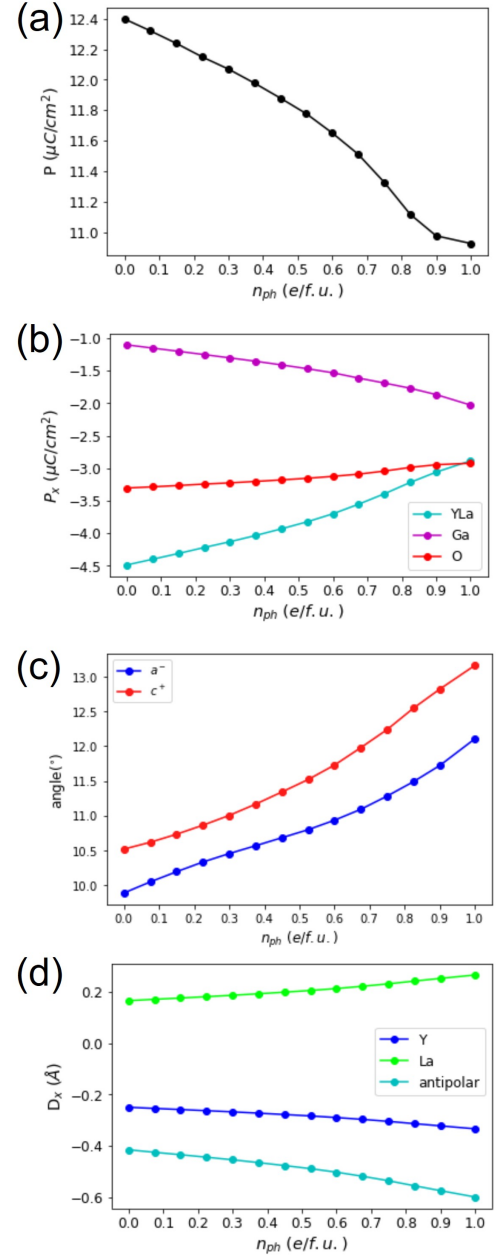


FIG. 2. Variations of different quantities with the number of photo-excited carriers  $n_{ph}$ . (a) Magnitude of polarization  $P$ . (b)  $P_x$  component contributed by A-site cations La and Y, Ga and oxygens, respectively. (c) The out-of-phase tilting ( $a^-$ ) angle and in-phase tilting ( $c^+$ ) angle. (d) The in-plane ionic displacement  $D_x^{\text{Y}}$ ,  $D_x^{\text{La}}$ , and antipolar displacement  $D_x^{\text{Y}} - D_x^{\text{La}}$ .

always opposite in sign) both increase in magnitude. Resultantly, the antipolar displacement  $D_x^{\text{Y}} - D_x^{\text{La}}$  also increases. This also results in a polarization approximated as:

$$P_x \sim D_x^{\text{Y}} + D_x^{\text{La}} \propto \phi_{a^-} \phi_{c^+} (K^{\text{Y}} - K^{\text{La}}), \quad (3)$$

which shows that apart from tilting amplitudes,  $P$  is also dependent on the coupling difference  $K^{\text{Y}} - K^{\text{La}}$ . Due to

mutual competition, this coupling difference is more delicate than their sum  $K^Y + K^{\text{La}}$ . The smaller  $P_x^{\text{YLa}}$  with increasing  $n_{\text{ph}}$  suggests that the two coupling strengths come closer to each other with an increasing illumination.

*Photo-induced mode coupling* To further understand the coupling between antipolar and non-polar tilting modes, we study phonons of the highly-symmetric  $P4/mmm$  tetragonal cell with one formula unit at different  $n_{\text{ph}}$ . The 10-atom,  $P4/mmm$  tetragonal cell is the parent of  $Pmc2_1$  structure (that has 20 atoms in its primitive cell). In combination with different tiltings and distortions, it can generate many descendent structures with lower symmetry. In essence, collective excitations of  $a^0a^0c^+$  and  $a^-a^-c^0$  tilting modes in real space correspond to unstable phonon modes at zone-boundary M point  $(1/2, 1/2, 0)$  of the  $P4/mmm$  tetragonal cell, and the antipolar modes correspond to the  $\Gamma$ -point modes at zone center  $(0, 0, 0)$  of this  $P4/mmm$  tetragonal cell. Phonon calculations are performed with the assistance of the Phonopy code [47]. Since notable photostriction was revealed in Fig. 1(c), we take half of the well-relaxed conventional orthorhombic lattice constants at different  $n_{\text{ph}}$  as the dimension of the tetragonal cell – implying that different volumes are used for the different chosen  $n_{\text{ph}}$  in these phonon computations. We refer to the SM for more details.

Frequencies of relevant modes are plotted in Figure 3. Note there are two antipolar modes, which are dominated by La and Y ions, respectively, and the La-dominant mode is stable. Results at dark condition are consistent with the previous study of Ref. [4] (see details in the SM). Though frequencies of two M-point modes increase with  $n_{\text{ph}}$ , they are still unstable at  $n_{\text{ph}} = 1\text{e/f.u.}$  with large imaginary wavenumbers. Also the increasing trend gets saturated at high  $n_{\text{ph}}$ . This also happens to the Y-dominant,  $\Gamma$ -point mode that the frequency is saturated at  $120i\text{ cm}^{-1}$  when  $n_{\text{ph}} = 1\text{e/f.u.}$ , while the frequency of La-dominant,  $\Gamma$ -point mode changes only slightly under illumination.

We write down a Landau free energy model to help understand the results of these phonon calculations:

$$F = \alpha_{M_1} X_{M_1}^2 + \beta_{M_1} X_{M_1}^4 + \alpha_{M_2} X_{M_2}^2 + \beta_{M_2} X_{M_2}^4 + \alpha_{\Gamma} X_{\Gamma}^2 + \beta_{\Gamma} X_{\Gamma}^4 + \gamma X_{M_1} X_{M_2} X_{\Gamma}. \quad (4)$$

In this model,  $X$  denotes the mode amplitude, and the subscript refers to each mode. Since  $M_1$ -,  $M_2$ - and  $\Gamma$ -point modes are unstable, it is necessary that their quadratic coefficients  $\alpha$  are negative, and their quartic coefficients  $\beta$  are positive. The last terms denote a trilinear coupling between three modes. Note that, in phonon calculations, the trilinear and quartic terms are not considered, as they are beyond second-order derivatives to energies within harmonic approximation. Typically, without trilinear coupling, the increasing frequency of an unstable mode denotes that the mode becomes

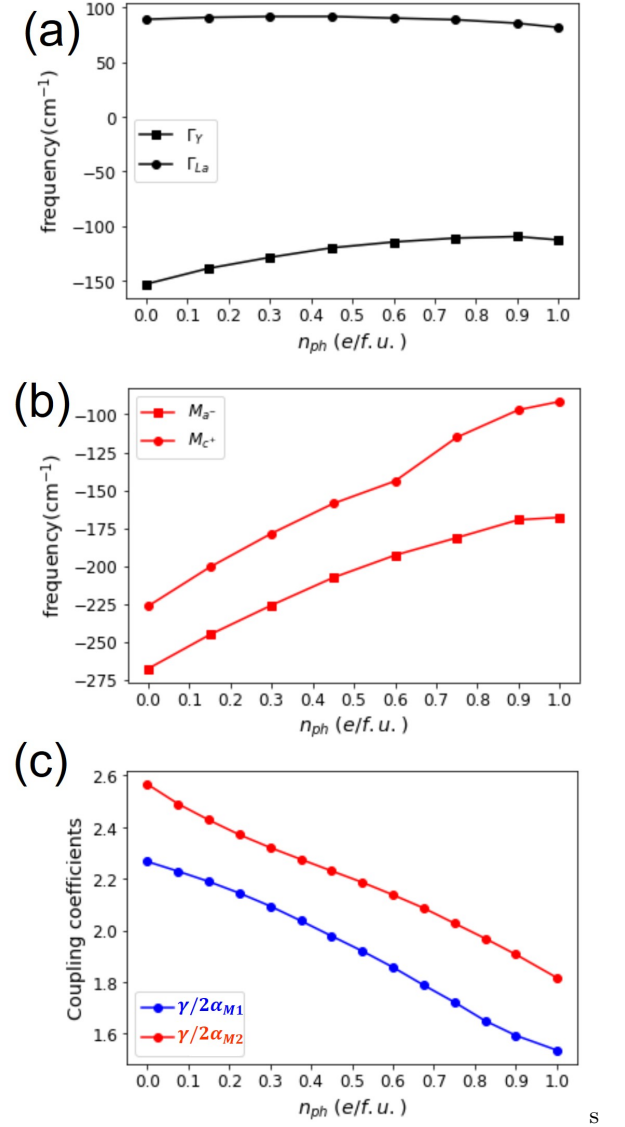


FIG. 3. Changes of phonon frequencies with  $n_{\text{ph}}$  in the parent tetragonal cell. (a) The Y-dominant and La-dominant antipolar modes at zone-center  $\Gamma$ -point  $(0, 0, 0)$ . (b) Modes at zone-boundary M-point  $(1/2, 1/2, 0)$  denoting  $a^-$  and  $c^+$  tiltings. (c) Changes of trilinear coupling coefficients  $\gamma/2\alpha_{M_{1,2}}$  with  $n_{\text{ph}}$  in the parent tetragonal cell.

more stable, and that will indicate a smaller tilting amplitude ( $\sqrt{|\alpha|/2\beta}$ ) with  $n_{\text{ph}}$ . However, Figs. 2(c) and (d) show an increase in tilting angles  $\phi$  and antipolar displacement  $\bar{D}^Y - \bar{D}^{\text{La}}$  with  $n_{\text{ph}}$ , contradicting the prediction from increasing frequencies of unstable modes. This can only be reconciled if the trilinear couplings are taken into account. Since tilting amplitudes can be approximated from the local minima of free energy  $F$  as  $X_{M_1} = |\gamma/2\alpha_{M_1}|X_{M_2}X_{\Gamma}$  and  $X_{M_2} = |\gamma/2\alpha_{M_2}|X_{M_1}X_{\Gamma}$ , we calculate the relative coupling coefficients  $\gamma/2\alpha_{M_{1,2}}$  from three mode amplitudes and plot them as a function of  $n_{\text{ph}}$  in Fig. 3(c). Anomalous behaviors of increasing



tilting angles but a decreasing polarization and hardening of tilting and antipolar modes reflects the critical role light plays in tuning couplings between modes, which further modifies mode amplitudes and affect resultant polarization.

*Discussion* Recent experiments show how polarization can be modified with above-bandgap ultrafast light. In the ferroelectric/dielectric superlattice  $\text{PbTiO}_3/\text{SrTiO}_3$ , polarization can be rotated towards the direction normal to the surface by the ultrafast laser pulse [48]. Reduction of in-plane and increase of out-of-plane polarization component are due to screening of the depolarization field by the photo-excited carriers. In  $\text{BaTiO}_3/\text{CaTiO}_3$  superlattice, lattice expansion in  $\text{BaTiO}_3$  and contraction in  $\text{CaTiO}_3$  is observed after the ultrafast optical excitation, indicating a polarization increase in  $\text{BaTiO}_3$  but decrease in  $\text{CaTiO}_3$  layer [49]. Recently in quantum paraelectric  $\text{KTaO}_3$ , a suppression of ferroelectricity is induced by photoexcitation, and has been attributed to hardening effect on transverse phonons [50]. Along with these experiments, our results indicate that hybrid improper ferroelectrics may be an alternative system that offers new ways to optically control ferroelectric polarization. Since the present system has a relatively large bandgap, the present work should also spur the search of new hybrid improper ferroelectric system with lower bandgaps in order to be able to use visible light.

The experiments discussed above pose an intriguing question whether the photo-induced polarization change is an electronic or structural effect. Our calculation shows that the photo-excited thermalized carriers cause a 3.5% in-plane and a 0.6% out-of-plane lattice expansion when  $n_{\text{ph}} = 1e/f.u.$ , and we wonder whether these structural effects fully account for the change of the polarization. To resolve this, we apply these strains on the lattice but under no light illumination and we then relax the internal atomic coordinates. As shown in the SM, in this way the total polarization decreases by 30%, which is more than twice the amount from the 12% decrease for an equal amount of strain but under illumination with  $n_{\text{ph}} = 1e/f.u.$  The different polarizations obtained in the two scenarios indicate that apart from the photostriction which deforms the lattice, electronic effect also plays an important role in photo-induced change on polarization, which aligns energy levels of photo-excited carriers by driving intrinsic ionic displacements and therefore altering polarization. More detailed analysis about polarization from each ion with/without light can be found in the SM.

*Conclusions* In summary, using first-principle calculations, we reveal that light can be an effective tool to manipulate ferroelectricity in hybrid-improper ferroelectric superlattices. We take the prototype system  $\text{LaGaO}_3/\text{YGaO}_3$  as an example and show, after photo-absorption, how polarization in the transient, quasi-equilibrium state varies with the number of photo-excited

thermalized carriers. A notable expansive photostriction is concomitantly observed, and the polarization change is achieved via controlling amplitudes of in-phase and out-of-phase tiltings, which are trilinearly coupled to A-site antipolar modes. Electronic effects associated with the occupation of thermalized carriers also contribute to the change of polarization. Recent studies show the availability to reorienting and tuning the magnitude of the polarization with the ultrafast laser pulse in ferroelectric oxides. Our study further demonstrates that (and explains why) light can be utilized as a powerful handle to govern exciting properties of functional materials in the future [50, 51].

We thank Bin Xu, Hong Jian Zhao and Peng Chen for useful discussions. L. G. and L. B. acknowledge the support from the Grant MURI ETHOS W911NF-21-2-0162 from Army Research Office (ARO). C.P. and L.B. thank ARO Grant No. W911NF-21-1-0113. L.G. acknowledges the support from the Arkansas High Performance Computing Center and HPCMP for computational resources. C.P. thanks the support from a public grant overseen by the French National Research Agency (ANR) as part of the “Investissements d’Avenir” program (Labex NanoSaclay, reference: ANR-10-LABX-0035) and the ANR Grant SUPERSPIN (No. ANR-21-CE24-0032).

- 
- [1] R. E. Cohen, Origin of ferroelectricity in perovskite oxides, *Nature* **358**, 136 (1992).
  - [2] E. Bousquet, M. Dawber, N. Stucki, C. Lichtensteiger, P. Hermet, S. Gariglio, J.-M. Triscone, and P. Ghosez, Improper ferroelectricity in perovskite oxide artificial superlattices, *Nature* **452**, 732 (2008).
  - [3] N. A. Benedek and C. J. Fennie, Hybrid improper ferroelectricity: a mechanism for controllable polarization-magnetization coupling, *Physical review letters* **106**, 107204 (2011).
  - [4] J. M. Rondinelli and C. J. Fennie, Octahedral rotation-induced ferroelectricity in cation ordered perovskites, *Advanced Materials* **24**, 1961 (2012).
  - [5] N. A. Benedek, A. T. Mulder, and C. J. Fennie, Polar octahedral rotations: a path to new multifunctional materials, *Journal of Solid State Chemistry* **195**, 11 (2012).
  - [6] W. Zhou and A. Ariando, Review on ferroelectric/polar metals, *Japanese Journal of Applied Physics* **59**, SI0802 (2020).
  - [7] K. J. Choi, M. Biegalski, Y. Li, A. Sharan, J. Schubert, R. Uecker, P. Reiche, Y. Chen, X. Pan, V. Gopalan, *et al.*, Enhancement of ferroelectricity in strained batio3 thin films, *Science* **306**, 1005 (2004).
  - [8] J. Haeni, P. Irvin, W. Chang, R. Uecker, P. Reiche, Y. Li, S. Choudhury, W. Tian, M. Hawley, B. Craigo, *et al.*, Room-temperature ferroelectricity in strained srtio3, *Nature* **430**, 758 (2004).
  - [9] T. Kolodiazny, M. Tachibana, H. Kawaji, J. Hwang, and E. Takayama-Muromachi, Persistence of ferroelectricity in batio 3 through the insulator-metal transition,

- Physical review letters **104**, 147602 (2010).
- [10] Y. Wang, X. Liu, J. D. Burton, S. S. Jaswal, and E. Y. Tsymbal, Ferroelectric instability under screened coulomb interactions, Physical review letters **109**, 247601 (2012).
  - [11] C. Xia, Y. Chen, and H. Chen, Coexistence of polar displacements and conduction in doped ferroelectrics: an ab initio comparative study, Physical Review Materials **3**, 054405 (2019).
  - [12] D. Hickox-Young, D. Puggioni, and J. M. Rondinelli, Persistent polar distortions from covalent interactions in doped batio 3, Physical Review B **102**, 014108 (2020).
  - [13] S. Li and T. Birol, Free-carrier-induced ferroelectricity in layered perovskites, Physical review letters **127**, 087601 (2021).
  - [14] Y. Shi, Y. Guo, X. Wang, A. J. Princep, D. Khalyavin, P. Manuel, Y. Michiue, A. Sato, K. Tsuda, S. Yu, *et al.*, A ferroelectric-like structural transition in a metal, Nature materials **12**, 1024 (2013).
  - [15] P. W. Anderson and E. Blount, Symmetry considerations on martensitic transformations: "ferroelectric" metals?, Physical Review Letters **14**, 217 (1965).
  - [16] Z. Fei, W. Zhao, T. A. Palomaki, B. Sun, M. K. Miller, Z. Zhao, J. Yan, X. Xu, and D. H. Cobden, Ferroelectric switching of a two-dimensional metal, Nature **560**, 336 (2018).
  - [17] A. Subedi, Proposal for ultrafast switching of ferroelectrics using midinfrared pulses, Physical Review B **92**, 214303 (2015).
  - [18] R. Mankowsky, A. von Hoegen, M. Först, and A. Cavalleri, Ultrafast reversal of the ferroelectric polarization, Physical review letters **118**, 197601 (2017).
  - [19] A. S. Disa, T. F. Nova, and A. Cavalleri, Engineering crystal structures with light, Nature Physics **17**, 1087 (2021).
  - [20] P. Chen, C. Paillard, H. J. Zhao, J. Íñiguez, and L. Bellaiche, Deterministic control of ferroelectric polarization by ultrafast laser pulses, Nature communications **13**, 1 (2022).
  - [21] C. Paillard, E. Torun, L. Wirtz, J. Íñiguez, and L. Bellaiche, Photoinduced phase transitions in ferroelectrics, Physical Review Letters **123**, 087601 (2019).
  - [22] V. Stoica, N. Laanait, C. Dai, Z. Hong, Y. Yuan, Z. Zhang, S. Lei, M. McCarter, A. Yadav, A. Damodaran, *et al.*, Optical creation of a supercrystal with three-dimensional nanoscale periodicity, Nature materials **18**, 377 (2019).
  - [23] M. Porer, M. Fechner, E. M. Bothschafter, L. Rettig, M. Savoini, V. Esposito, J. Rittmann, M. Kubli, M. J. Neugebauer, E. Abreu, *et al.*, Ultrafast relaxation dynamics of the antiferrodistortive phase in ca doped sr tio 3, Physical review letters **121**, 055701 (2018).
  - [24] M. Porer, M. Fechner, M. Kubli, M. J. Neugebauer, S. Parchenko, V. Esposito, A. Narayan, N. Spaldin, R. Huber, M. Radovic, *et al.*, Ultrafast transient increase of oxygen octahedral rotations in a perovskite, Physical Review Research **1**, 012005 (2019).
  - [25] A. Kogar, A. Zong, P. E. Dolgirev, X. Shen, J. Straquadine, Y.-Q. Bie, X. Wang, T. Rohwer, I. Tung, Y. Yang, *et al.*, Light-induced charge density wave in late3, Nature Physics **16**, 159 (2020).
  - [26] G. Marini and M. Calandra, Light-tunable charge density wave orders in mote 2 and wte 2 single layers, Physical review letters **127**, 257401 (2021).
  - [27] C. Paillard, B. Xu, B. Dkhil, G. Geneste, and L. Bellaiche, Photostriction in ferroelectrics from density functional theory, Physical Review Letters **116**, 247401 (2016).
  - [28] C. Paillard, S. Prosandeev, and L. Bellaiche, Ab initio approach to photostriction in classical ferroelectric materials, Physical Review B **96**, 045205 (2017).
  - [29] R. Haleoot, C. Paillard, T. P. Kaloni, M. Mehboudi, B. Xu, L. Bellaiche, and S. Barraza-Lopez, Photostrictive two-dimensional materials in the monochalcogenide family, Physical review letters **118**, 227401 (2017).
  - [30] S. Sarkar, I.-W. Un, Y. Sivan, and Y. Dubi, Theory of non-equilibrium hot carriers in direct band-gap semiconductors under continuous illumination, arXiv preprint arXiv:2110.12818 (2021).
  - [31] J. Fast, U. Aeberhard, S. P. Bremner, and H. Linke, Hot-carrier optoelectronic devices based on semiconductor nanowires, Applied Physics Reviews **8**, 021309 (2021).
  - [32] A. Othonos, Probing ultrafast carrier and phonon dynamics in semiconductors, Journal of applied physics **83**, 1789 (1998).
  - [33] D. König, K. Casalenuovo, Y. Takeda, G. Conibeer, J. Guillemoles, R. Patterson, L. Huang, and M. Green, Hot carrier solar cells: Principles, materials and design, Physica E: Low-dimensional Systems and Nanostructures **42**, 2862 (2010).
  - [34] A. R. Attar, H.-T. Chang, A. Britz, X. Zhang, M.-F. Lin, A. Krishnamoorthy, T. Linker, D. Fritz, D. M. Neumark, R. K. Kalia, *et al.*, Simultaneous observation of carrier-specific redistribution and coherent lattice dynamics in 2h-mote2 with femtosecond core-level spectroscopy, ACS nano **14**, 15829 (2020).
  - [35] D. M. Fritz, D. Reis, B. Adams, R. Akre, J. Arthur, C. Blome, P. Bucksbaum, A. L. Cavalieri, S. Engemann, S. Fahy, *et al.*, Ultrafast bond softening in bismuth: mapping a solid's interatomic potential with x-rays, Science **315**, 633 (2007).
  - [36] E. G. Gamaly, The physics of ultra-short laser interaction with solids at non-relativistic intensities, Physics Reports **508**, 91 (2011).
  - [37] H. Yasuda, Y. Yamada, T. Tayagaki, and Y. Kanehitsu, Spatial distribution of carriers in sr tio 3 revealed by photoluminescence dynamics measurements, Physical Review B **78**, 233202 (2008).
  - [38] P. Tangney and S. Fahy, Calculations of the a 1 phonon frequency in photoexcited tellurium, Physical review letters **82**, 4340 (1999).
  - [39] E. Murray, D. Fritz, J. Wahlstrand, S. Fahy, and D. Reis, Effect of lattice anharmonicity on high-amplitude phonon dynamics in photoexcited bismuth, Physical Review B **72**, 060301 (2005).
  - [40] A. M. Glazer, The classification of tilted octahedra in perovskites, Acta Crystallographica Section B: Structural Crystallography and Crystal Chemistry **28**, 3384 (1972).
  - [41] X. Gonze, B. Amadon, P.-M. Anglade, J.-M. Beuken, F. Bottin, P. Boulanger, F. Bruneval, D. Caliste, R. Caracas, M. Côté, *et al.*, Abinit: First-principles approach to material and nanosystem properties, Computer Physics Communications **180**, 2582 (2009).
  - [42] B. Peng, D. Bennett, I. Bravić, and B. Monserrat, Tunable photostriction of halide perovskites through energy dependent photoexcitation, arXiv preprint

- arXiv:2206.00061 (2022).
- [43] A. Narayan, Effect of strain and doping on the polar metal phase in  $\text{LiOsO}_3$ , *Journal of Physics: Condensed Matter* **32**, 125501 (2019).
  - [44] A. T. Mulder, N. A. Benedek, J. M. Rondinelli, and C. J. Fennie, Turning  $\text{ABO}_3$  antiferroelectrics into ferroelectrics: design rules for practical rotation-driven ferroelectricity in double perovskites and  $\text{A}_2\text{B}_2\text{O}_7$  ruddlesden-popper compounds, *Advanced Functional Materials* **23**, 4810 (2013).
  - [45] H. J. Zhao, J. Iniguez, W. Ren, X. M. Chen, and L. Bellaiche, Atomistic theory of hybrid improper ferroelectricity in perovskites, *Physical Review B* **89**, 174101 (2014).
  - [46] L. Bellaiche and J. Iniguez, Universal collaborative couplings between oxygen-octahedral rotations and antiferroelectric distortions in perovskites, *Physical Review B* **88**, 014104 (2013).
  - [47] A. Togo and I. Tanaka, First principles phonon calculations in materials science, *Scripta Materialia* **108**, 1 (2015).
  - [48] H. J. Lee, Y. Ahn, S. D. Marks, E. C. Landahl, S. Zhuang, M. H. Yusuf, M. Dawber, J. Y. Lee, T. Y. Kim, S. Unithrattil, *et al.*, Structural evidence for ultrafast polarization rotation in ferroelectric/dielectric superlattice nanodomains, *Physical Review X* **11**, 031031 (2021).
  - [49] D. Sri Gyan, H. J. Lee, Y. Ahn, R. B. Carson, J. Carnis, T. Y. Kim, S. Unithrattil, J. Y. Lee, S. H. Chun, S. Kim, *et al.*, Optically induced picosecond lattice compression in the dielectric component of a strongly coupled ferroelectric/dielectric superlattice, *Advanced Electronic Materials*, 2101051 (2021).
  - [50] V. Krapivin, M. Gu, D. Hickox-Young, S. Teitelbaum, Y. Huang, G. de la Peña, D. Zhu, N. Sirica, M.-C. Lee, R. Prasankumar, *et al.*, Ultrafast suppression of the ferroelectric instability in  $\text{KtAO}_3$ , *Physical review letters* **129**, 127601 (2022).
  - [51] C. Zhang, C. Song, Q. Yang, X. Liu, H. Zhao, and S. Meng, Electronic origin of ultrafast laser-induced ferroelectricity in  $\text{SrTiO}_3$ , (unpublished) (2022).